Surface interaction between metallic cobalt and tungsten carbide particles as a primary cause of hard metal lung disease

Giovanna Zanetti and Bice Fubini

Dipartimento di Chimica Inorganica, Chimica Fisica e Chimica dei Materiali, Università di Torino, via P. Giuria 7, 10125 Torino, Italy

Hard metal dusts, typically WC/Co, but not pure WC or Co particles, cause the so-called 'hard metal lung disease' when inhaled over long periods of time at the workplace. In order to investigate the chemical nature of the dust which originates the disease, the surface behaviour of pure cobalt, pure tungsten carbide, an industrial hard metal dust and a mechanical mixture of cobalt and tungsten carbide have been compared. Electron microscopy reveals an intimate contact between metal and carbide in the mixed dusts. The mixed dust is more active than the single components in the adsorption of water vapour in both adsorbed amount and interaction energy (111 kJ mol^{-1} for the mixture, 95 kJ mol^{-1} for pure cobalt and 84 kJ mol^{-1} for pure WC). Both industrial and mechanical mixtures are more active than pure components in the catalytic decomposition of hydrogen peroxide. Incubation of the mixed dusts in phosphate buffered solutions causes a progressive release of cobalt(II) ions in solution and the appearance of round smooth aggregates (diameter *ca.* 300–400 μm) at the expense of smaller particles. The mixed dusts, but not the pure components, promote the homolytic rupture of a carbon–hydrogen bond in aqueous suspension, as revealed by the formation of carboxylate radicals from formate ions. This is evidenced by the use of DMPO as a spin trap, which yields the DMPO$-CO_2^{\cdot -}$ adduct whose EPR spectrum intensity measures the amount of radicals generated. Radicals are only formed in aerated solutions indicating a crucial role of atmospheric oxygen in their generation. The hydroxyl radical, however, does not appear to be implied, for two main reasons: (i) no free oxygen radicals are detected in the absence of formate as target molecule; and (ii) free-radical release is insensitive to the addition of mannitol (an $^{\cdot}OH$ scavenger). The formation of the carboxylate radical $CO_2^{\cdot -}$ is an activated process: an induction time of *ca.* 30 min is required to produce detectable amounts of radicals, while radical generation continues for several hours. Samples withdrawn from the solution, washed, dried and re-employed are still active, as long as some metallic cobalt is present. A model is proposed whereby in the mixture electrons from oxidized cobalt are translocated at the carbide surface where they reduce atmospheric oxygen in a surface-active form which is responsible for the generation of carboxylate radicals from formate ions. The implication of this reaction in health related effects as well as possible hazards from particulates in enviromental pollution is discussed.

Hard metals are present in a intimate mixture of metallic and carbide particles.[1] They are largely employed in manufacturing sharp edges such as saw blades, cutters, drill bits and some armament components.

Hard metals, derived from the association of tungsten carbide and cobalt, have widespread use and are the most investigated from the standpoint of their health effects.[2–4] Workers exposed to WC/Co dusts for long periods of time are often afflicted by an occupational disease, termed hard metal lung disease, which does not afflict people exposed to each single component, *i.e.* cobalt metal particles or tungsten carbide dusts.[2,5,6] Epidemiological data, reviewed and discussed in ref. 6, suggest in fact that the risk is high among hard metal workers and diamond polishers but unusual or even absent when exposure is to pure cobalt dust, *e.g.*, in cobalt refinery plants.

Several *in vivo* and *in vitro* tests have shown that the biological response to the mixture is different from that to the single components.[7–10] It appears therefore that the origin of the disease has to be sought in a particular chemical reaction, which takes place only in the presence of the two components. This would then trigger a series of other reactions ending up with the pathogenic response to the particulate.

The molecular mechanism underlying this process has already been investigated in this laboratory.[11] A consistent free-radical release was evidenced by means of the spin-trapping technique. A model was proposed whereby atmospheric oxygen was activated in aqueous buffered suspensions of the mixed dust with consequent oxidation of cobalt and release of cobalt ions into solution. During this reaction electron donation from cobalt to dissolved oxygen would generate oxygen-based radicals. Reactive oxygen species (ROS) are highly toxic and are known to cause DNA damage and lipid peroxidation in *in vitro* assays which may initiate a pathogenic mechanism; they have recently been considered one of the most probable causes of asbestos associated diseases.[12] Their implication also in some phases of the development of hard metal lung disease is thus quite plausible.

The association of cobalt ions with tungsten carbide was inactive in radical release suggesting that the reactivity of the mixed dusts originates at the interface between the two solid phases and not from the reaction of a solubilized component at the solid surface.

Some chemical aspects need, however, still to be clarified, such as the chemical nature of the reactive oxygen species, the redox mechanism taking place, the kinetics of free radical release and the evidence for a long lasting mechanism, as required to explain toxicity.

The present paper reports new results on the reactivity of cobalt–tungsten carbide mixtures, namely: (*i*) investigations on free-radical release from the mixture and from single components by means of the spin-trapping technique. This technique involves an addition reaction of short-lived free radicals with a diamagnetic compound to form a relatively long-lived paramagnetic adduct which is studied by electron paramagnetic resonance (EPR) spectroscopy. Tests have been performed: (*a*) in the absence and in the presence of formate as a target molecule, in order to evaluate the presence of the hydroxyl radical, if any; (*b*) in the presence of hydrogen peroxide in order to evidence a Fenton mechanism; (*c*) in subsequent tests on the same sample, to clarify whether or not radicals are released *via* a catalytic reaction and (*d*) by recording at different

times the amount of radicals formed, *i.e.* the kinetics of the process taking place.

(*ii*) A morphological study by scanning electron microscopy (SEM) of the state of the solid during reaction and by energy dispersive spectrometry (EDS) in order to evaluate the variations in chemical composition of the outermost layers of the particles during incubation in aqueous solutions.

(*iii*) An evaluation of the affinity for water of the mixture compared to those of the single components, measured calorimetrically from the heat of adsorption of water vapour.

(*iv*) A measure of the catalytic activity of the mixture and of the single components in the disproportionation of hydrogen peroxide in aqueous solution.

Experimental

Materials

Solids. The samples employed were the same as those previously used in *in vivo* and *in vitro* tests, described in ref 6, 7 and 10: extra-fine cobalt metal powder (99.7%, $d_{50}=4$ μm); tungsten carbide (Johnson Matthey 62655, 99.5%, $d_{50}<1$ μm), denoted WC_{JM}; hard metal powder obtained from a production factory before paraffin addition and sintering [6.3 mass% of extra-fine cobalt metal particles; 89.4 mass% tungsten carbide particles and 1.5 mass%, iron $d_{50}=2$ μm], denoted WC/Co; a mixture of the pure two mayor components (WC, Co) prepared in the laboratory without extensive milling, denoted reconstructed WC/Co (rWC/Co); tungsten carbide obtained treating the industrial WC/Co mixture for 12 h with 37% HCl, washing with distilled water and drying, denoted WC_{HCl}. By this procedure all metal particles and oxides are dissolved, leaving the original WC particles virtually unaltered.

Surface areas of the samples employed measured by the BET method (nitrogen adsorption at −196 °C, 'Quantasorb' Quantacrome), are given in Table 1.

WC_{HCl} was employed in all tests (*e.g.* adsorption calorimetry), where a similar morphology of the particles and a reasonable surface area were required. WC_{JM} was instead employed when an extremely pure metal-free sample was required to compare mixtures and single component behaviour, *i.e.* in the detection of free-radical release and in the study of the catalytic decomposition of hydrogen peroxide.

Chelex 100, a chelating resin (iminodiacetic acid), was from Sigma.

Chemicals. 5,5-Dimethyl-1-pyrroline *N*-oxide (DMPO, Fluka Buchs, Switzerland) was used as a spin-trapping agent. To minimise contamination by degradation products and metal ions, DMPO was first dissolved in Chelex-treated water, purified by passing through charcoal, and stored in the dark.

Sodium formate, used as the target molecule for free-radical generation, was from Sigma. 0.5 M HPO_4^{2-}–0.5 M $H_2PO_4^-$ (Merk) was employed for the phosphate buffer (pH = 7.4). H_2O_2 was from Fluka.

Titration of H_2O_2 was performed *via* an enzymatic method[13] employing peroxidase (Sigma) and leuco crystal violet (Sigma) in acetate buffer (acetic acid and sodium acetate, Fluka).

The water vapour employed in adsorption calorimetry was obtained by water distilled several times *in vacuo* and rendered gas-free by several freeze–pump–thaw cycles.

Table 1 Specific surface area of the samples

sample	surface area (BET)/$m^2\ g^{-1}$
Co	1.1
WC_{JM}	0.1
WC_{HCl}	2.3
WC/Co	2.0

Methods

Evaluation of free-radical generation by means of the spin-trapping technique. The potential of the various dust samples in generating free radicals was evaluated by means of the spin-trapping technique[14,15] applied to the aqueous particulate suspensions. The procedure adopted, first reported by Zalma *et al.*,[16] has been already employed in our laboratory in the study of iron-containing materials.[17] DMPO is used to stabilise otherwise short-lived radicals, allowing a nearly quantitative evaluation of the amount of free radicals present in the suspension, through the intensity of the EPR spectra of the DMPO adducts with the radicals.

Two different tests were performed. A first test, designated A–OH, reveals the presence of $^{\cdot}OH$ radicals by the formation of the DMPO−$OH^{\cdot}$ adduct following the reaction:

$$DMPO + {}^{\cdot}OH \rightarrow DMPO-OH^{\cdot}$$

The detailed protocol was as follows: 45 mg of particles were weighed in a glass vessel into which were introduced 2 ml of Chelex-treated 0.5 M phosphate buffer (pH 7.4) and 0.05 M DMPO. The reaction mixture was then incubated in the dark for 5 or 25 min (37 °C) under vigorous agitation, and 1 ml of the liquid phase was withdrawn, filtered (0.65 μm pores), and transferred into a flat quartz EPR cell.

The more widely used test, designated F–C, employs formate as the target molecule:[16] the potential for causing a homolytic rupture of a carbon–hydrogen bond is evaluated through the amount of $CO_2^{\cdot -}$ radicals formed following hydrogen abstraction from a formate anion. This reaction may be caused by hydroxyl radicals or by other highly electrophilic species in solution or at the solid/liquid interface.

The reaction taking place may be summarised as follows:

$$X + HCO_2^- \rightarrow CO_2^{\cdot -} + HX$$

where X may be either an active site at the solid surface itself or a previously formed reactive radical (*e.g.* $^{\cdot}OH$)

$$DMPO + CO_2^{\cdot -} \rightarrow DMPO-CO_2^{\cdot -}$$

The sequence of operations is similar to that for the A–OH test, except that longer times of incubation before withdrawing the supernatant aliquots from the suspensions were employed because of the higher stability of the DMPO−$CO_2^{\cdot -}$ adduct.[15]

45 mg of particles were weighed in a glass vessel to which was added 2 ml of Chelex-treated 1 M phosphate buffer (pH 7.4) containing 1 M sodium formate and 0.05 M DMPO. The reaction mixture was then incubated in the dark for 25 or 55 min (37 °C) under vigorous agitation, and 1 ml of the liquid phase was withdrawn, filtered (0.65 μm), and transferred into a quartz EPR flat cell. The same test was performed in the absence of oxygen, *i.e.* under a nitrogen atmosphere.

The intensity of the DMPO−$OH^{\cdot}$ and of the DMPO−$CO_2^{\cdot -}$ signal were expressed in arbitrary units (arb. units) calculated by dividing the height of the signal (S in mm) by the receiver gain (RG) [arb. unit = (100 S)/RG]. One arbitrary unit corresponds to *ca.* 1×10^{15} spin ml^{-1}.

Blanks were made by operating in the same way in the absence of solid particulate in the solution. Because of an intrinsic variability in activity from one DMPO preparation to another, blank tests and standard tests with an active dust were performed before each set of experiments.

The F–C test was also performed in the presence of mannitol, a well known scavenger of hydroxyl radicals. Different amounts of mannitol were added to the DMPO–formate solution.

In order to investigate the catalytic nature of the process, the F–C test was performed subsequently on the same sample by thorough washing and drying the dust after the first test.

The kinetics of free-radical generation were evaluated by performing the reaction as described for the F–C test, but in this case 1 ml of the liquid phase was withdrawn, filtered and

transferred into a flat quartz EPR cell at different subsequent times and the spectra recorded.

All EPR spectra were recorded on a Varian E109 spectrometer at a microwave power of 10 mW, scan range 100 G, and a modulation amplitude of 1 G.

Evaluation of the release of cobalt ions from buffered aqueous suspension. The release of cobalt ions from aqueous suspensions of Co and WC/Co powders were measured under the same conditions (aqueous suspension of the dust in phosphate buffer, 37 °C, agitation) as in the spin-trapping studies. After 1 and 5 min, an aliquot of the suspension was withdrawn and filtered (filter pore diameter = 0.45 μm). The amount of solubilized cobalt was measured by a double beam spectrophotometer (UVIKON 930) at 530 nm, which is the wavelength of the maximum absorption of $CoCl_2$ solubilized in phosphate buffer (1 M). The spectrum of the cobalt ions originating from Co and WC/Co was similar to $CoCl_2$ and different from that reported for cobalt(III) salts. The amount of cobalt ions extracted from the dust could be accurately measured only at very low concentration in the buffered solution because of the low value of the solubility product of cobalt phosphate [$Co_3(PO_4)_2$ $K_s = 2.05 \times 10^{-35}$ at 25 °C].

Adsorption calorimetry. The adsorption of water vapour on the various samples was evaluated by means of a Tian-Calvet microcalorimeter (Setaram), connected to a vacuum/gas volumetric apparatus extensively described in previous papers.[18,19]

The samples, placed in the calorimetric cell, were pre-treated *in vacuo* at 423 K for 2 h and subsequently transferred into the calorimeter without further exposure to the atmosphere. Adsorption was performed in all cases at 303 K; small doses of the adsorbant were subsequently admitted onto the sample, the sample being continuously monitored by means of a 0–100 Torr (1 Torr ≈ 133 Pa) transducer gauge (Baratron MKS).

The procedure for each adsorption cycle was as follows: (*i*) adsorption of successive doses of the adsorbant, up to an established equilibrium pressure limit (*ca.* 5 Torr), on the fresh sample (ads I); (*ii*) desorption by direct evacuation of the sample until no deviation on the calorimetric baseline was detectable; (*iii*) adsorption of doses similar to those in ads I up to the same equilibrium pressure, in order to evaluate the fraction of the adsorbate which is reversibly adsorbed at the adopted adsorption temperature (ads II).

Electron microscopy. High-resolution transmission electron microscopy (HRTEM) micrographs were obtained with a JEOL JEM 2000 EX electron microscope (200 kV acceleration), equipped with a top-entry stage: the samples were dispersed in *n*-heptane and then deposited on Cu grids coated with a porous carbon film.

Scanning electron microscopy (SEM) micrographs and scanning electron microscope equipped for energy dispersive spectrometry (SEM–EDS) elemental analysis were obtained with an Oxford Link electron microscope.

Samples were examined as received and after incubation in aqueous-buffered solutions. In the latter case the dust was recovered by filtering, washing several times and then drying.

Kinetics of decomposition of H_2O_2. 1 ml of 0.1 M hydrogen peroxide and 30 ml of distilled water were added to 50 mg of the sample and then incubated at 37 °C and shaken in the dark. Aliquots of the suspension (100 μl) were withdrawn at subsequent times: (10, 30, 60, 120, 240 and 300 min) and then filtered through 20 nm porosity filters. The residual undecomposed hydrogen peroxide in solution was determined in the filtrate by an enzymatic assay whereby peroxidase catalyses the oxidation of a substrate (leuco crystal violet) by H_2O_2, following a method described by Mottola *et al.*,[13] already employed with iron-containing dust suspensions.[17]

Blanks were made operating in the same way except that no solid particulate was introduced into the solution. In order to calculate the % H_2O_2 decomposed by the catalytic reaction, the value of [H_2O_2] of the blank at all times has been considered as the actual H_2O_2 concentration which would be in the solution in the absence of any catalyst.

Results

Micromorphology of the dust particles

Fig. 1 shows images of WC_{HCl} and WC/Co obtained by HRTEM. Fig. 1(*a*) shows details of a single WC_{HCl} particle. The edges are clearly very smooth and the contours are very regular. Fig. 1(*b*) shows a micrograph of WC/Co at the same magnification as in Fig. 1(*a*). In this case the edges are irregular and indented. As WC_{HCl} was obtained by leaching WC/Co with HCl solution, which does not react with the carbide, the differences found between WC/Co and WC_{HCl} are simply assigned to the presence of Co. The micromorphology evidenced in Fig. 1(*b*) suggests that, in the mixture, cobalt is somehow 'spread' on the WC surface, causing the irregular aspects of the surface edges.

SEM micrographs of WC_{JM}, Co, WC/Co and rWC/Co samples [Fig. 2(*a*)–(*d*)] are similar to each other and at the magnification attained by SEM, the details of surface irregularities evidenced by TEM are not visible. In the WC/Co and rWC/Co samples (Fig. 2), however, it is possible to evidence a few aggregates with dimensions around 50 μm, indicated by an arrow in Fig. 2(*c*), (*d*), which are not present in the pure components.

The industrial and the reconstructed mixtures used for EPR

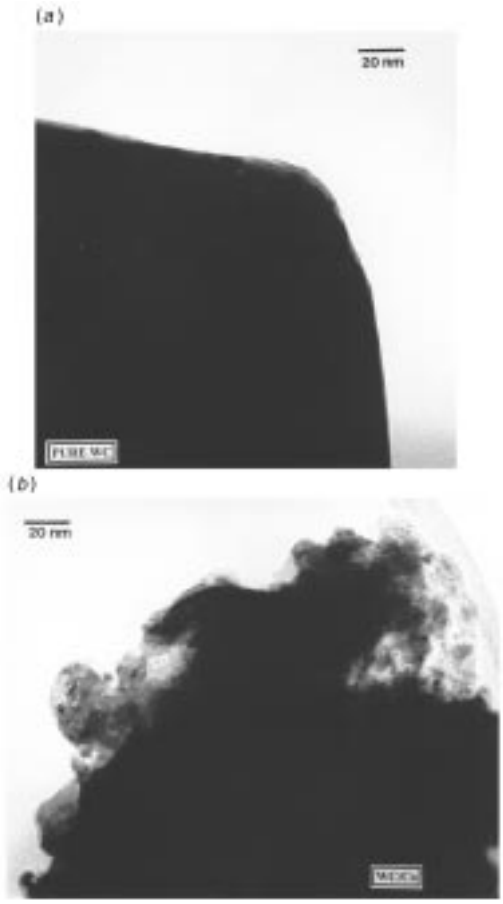

Fig. 1 Transmission electron microscopy images of WC_{HCl} (*a*) and of WC/Co (*b*)

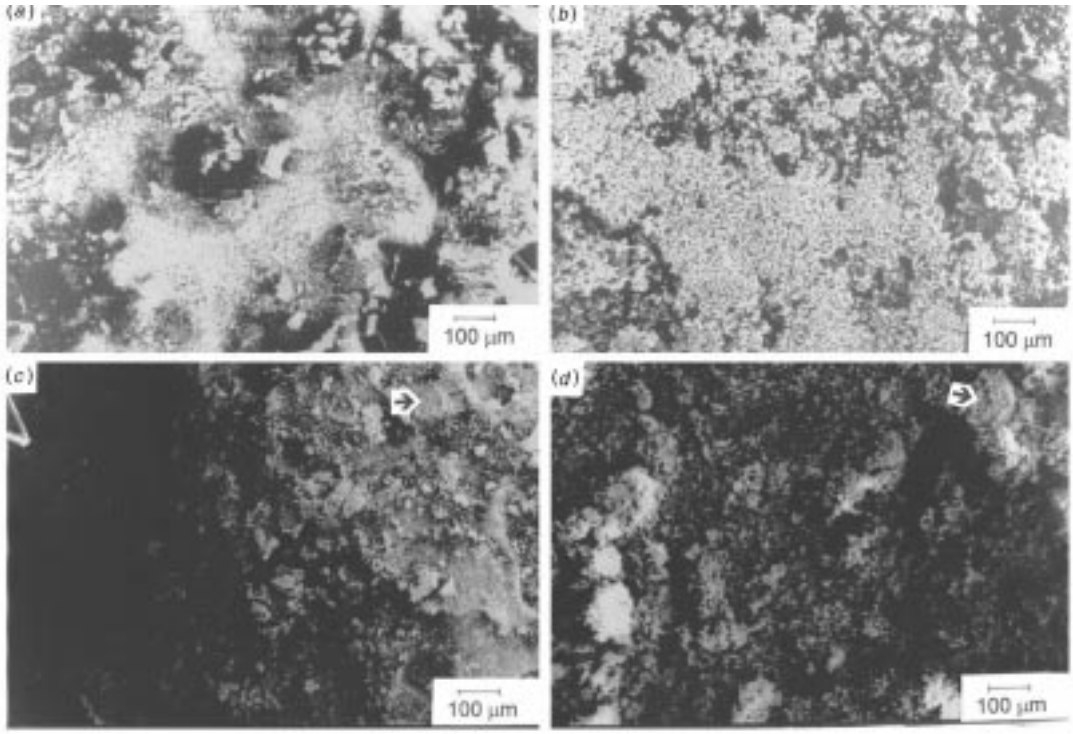

Fig. 2 Scanning electron microscopy images of the original samples: (*a*) WC_{JM}, (*b*) Co, (*c*) WC/Co, (*d*) rWC/Co

experiments (incubated for *ca.* 60 min in a phosphate-buffered solution containing formate and the spin trap) were recovered from the suspension, dried and examined by SEM. The micrographs [Fig. 3(*a*), (*b*)] reveal more aggregates than in the starting materials, which are larger and appear as round and smooth particles with sizes in the range 100–400 μm.

In some cases EPR experiments were performed several times on the same solid and after each measurement the solid particulate was filtered and dried. The corresponding SEM images (not shown) show a larger amount of these large rounded aggregates and reveal that the original small particles have been progressively consumed. After three subsequent tests virtually all the small particles had disappeared.

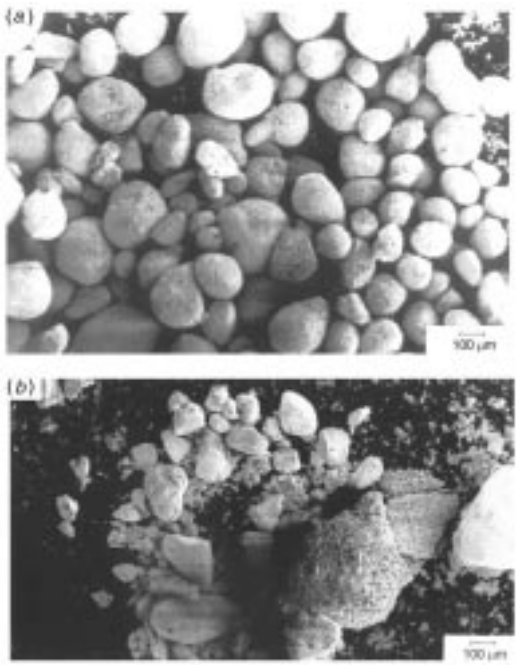

Fig. 3 Scanning electron microscopy images of samples, incubated for 60 min in the phosphate-buffered solution used for spin-trapping measurements (containing formate and DMPO), recovered from the suspension and dried: (*a*) WC/Co, (*b*) rWC/Co

In order to follow the progressive transformation from the original sample to the sample mostly constituted of large particles, SEM images have been recorded on samples of pure cobalt and of the industrial mixture extracted from the suspension after 2, 5, 15, 30 or 60 min. The results on both Co and WC/Co samples are shown in Fig. 4(*a*)–(*e*) (cobalt) and 4(a_1)–(e_1) (industrial mixture).

A separate suspension was prepared for each time, in order to avoid any modification due to removal of a part of the liquid phase from the system, which could alter the equilibrium established in solution at the solid/liquid interface.

The pure cobalt samples are mostly constituted of a finely divided dust with very few aggregates with dimensions between 50 and 100 μm. The sample incubated for 60 min exhibits a few more aggregates than the others. By contrast, the WC/Co samples show the presence of many large smooth aggregates even after only 2 min of incubation, the number of which increases with incubation time. The large particles are in the range 300–400 μm, while the number of small particles progressively decreases.

Because of the procedure adopted, any artefact related to loss of small particles during successive filtrations can be ruled out, thus the change with incubation time is due to progressive modification of the particulate size and composition.

A detailed crystallochemical analysis of these rounded aggregates is beyond the aim of this paper. Comparison between the two series of images, however, reveals that in the mixture the aggregating agent, probably cobalt/phosphate complexes, is much more active than in the suspension of pure cobalt particles.

Evaluation of the release of cobalt ions in the suspension

(a) Cobalt in the solid mixture. SEM–EDS analysis on the WC/Co sample, recovered from successive incubations in a phosphate/formate buffered solution, shows that the amount of cobalt present in the solid mixture progressively decreases

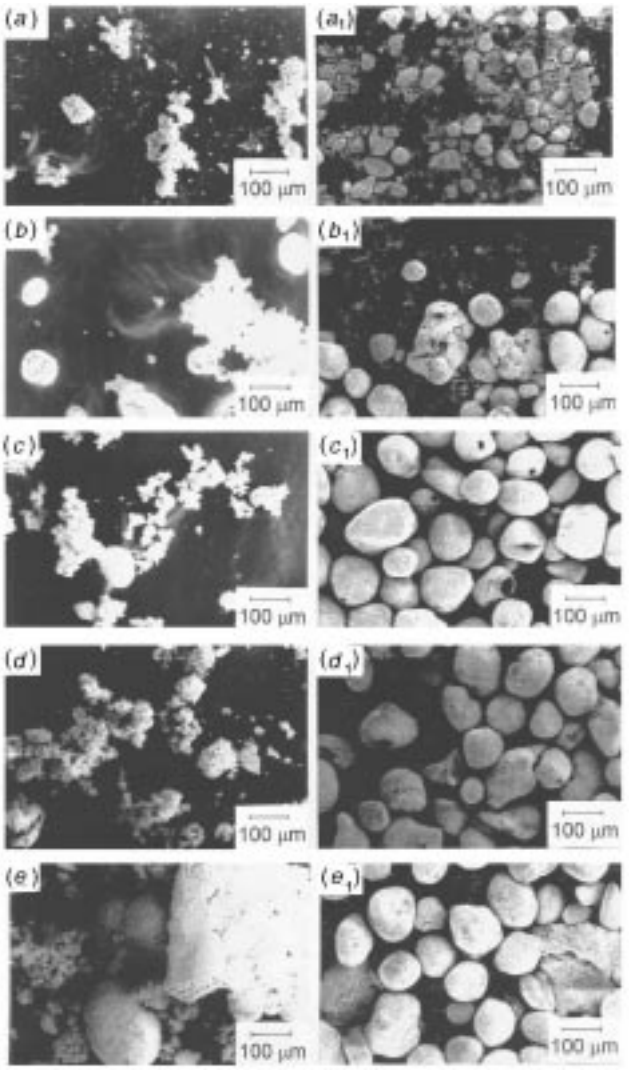

Fig. 4 Scanning electron microscopy images of Co (*a–e*) and WC/Co (a_1–e_1) samples incubated in a phosphate-buffered solution containing formate and DMPO, recovered from the suspension at the following times: 2 (*a*, a_1), 5 (*b*, b_1), 15 (*c*, c_1), 30 (*d*, d_1), 60 min (*e*, e_1) and subsequently dried

in subsequent tests. After the first incubation the amount of cobalt is reduced to a third of the original value and at the end of the two tests no cobalt is detectable.

(b) Cobalt oxidized and brought into solution. All dust suspensions are pink, the intensity of the colour increases with time of incubation, which indicates that some cobalt has been oxidized and brought into solution. Some cobalt ions were released in solution immediately after suspension of the particles in the buffered solutions. This amount was higher for WC/Co than for a quantity of pure cobalt equal to that present in the mixture, in accord with previous results.[11]

For incubation times >2 min the concentration of cobalt in solution varies in both cases in a complex manner. This is due to the interplay of different complexation and precipitation equilibria taking place in the suspensions. Under these conditions the concentration of cobalt measured spectrophotometrically underestimates the amount of cobalt actually extracted from the original solid phase, since microprecipitates and some complexes elude detection.

Heat of adsorption of water vapour

Fig. 5(*a*) and (*b*) show volumetric and calorimetric isotherms,[18] respectively, for the total adsorption of water (ads I) on the sample outgassed at 150 °C and Fig. 5(a_1) and (b_1) for the reversible adsorption of water (ads II) on WC_{HCl}, Co and WC/Co. Uptake values, integral heats and the molar heats measured at an equilibrium pressure of 5 Torr are listed in Table 2.

Water uptake, measured per unit surface, is much larger in the entire pressure range examined on Co than on WC_{HCl}. Comparison at the same equilibrium pressure (*e.g.* 5 Torr, see Table 2) reveals that the amount of water adsorbed on cobalt is nearly twice that adsorbed on the carbide, 10.2 molecule nm^{-2} for cobalt and 5.5 molecule nm^{-2} for tungsten carbide.

The higher affinity of water for cobalt than for the carbide may be attributed to a thin oxide external layer present on the surface of the metal particles, which probably imparts a high polarity and hydrophilicity to the surface.

The amount of water adsorbed (ads I) on WC/Co is midway between the uptake on Co and on WC_{HCl}, despite the relatively high amount of WC (89%) and low amount of Co (6%) contained in the mixture. The amount of water, which would have been adsorbed if the two components acted independently, is much below the experimental values in the entire range (0–10 Torr) examined (Table 2).

It is clear that the experimental values exceed the calculated values indicating that activation of cobalt in the mixture has taken place, *i.e.* the mixture behaves as if the cobalt/cobalt oxide external layer much exceeded the extent of surface coverage on a geometrical basis. This activation leads to surface sites which adsorb water vapour irreversibly. The isotherm related only to reversible adsorption [Fig. 5(*a*), (*b*); ads II] by contrast does not reveal such an enhancement in heat and adsorption values in the mixture.

When comparing the heat effects (Table 2), the differences between experimental and calculated values is even more pronounced. The trends are similar to the volumetric measurements, but the WC/Co curve lies much closer to that for pure cobalt indicating that not only are some sites activated in the mixture but that they also exhibit a higher energy than those in the pure components. The molar heat for the mixture (Table 2), accordingly, not only is higher than that expected if there were no interactions between components, but also exceeds the value for pure cobalt by *ca.* 15 kJ mol^{-1}.

The evolution of the heat of adsorption of water vapour with coverage (not shown for the sake of brevity) shows that Co, WC_{HCl} and WC/Co are all fully hydrophilic, as the interaction with water exhibits an energy higher than the latent heat of liquefaction (44 kJ mol^{-1}) in the whole range examined.[20] The degree of hydrophilicity increases in the order WC $<$ Co $<$ WC/Co.

Catalytic activity in the decomposition of hydrogen peroxide

The ability of Co, WC_{JM}, WC/Co and rWC/Co to act as heterogeneous catalysts for the decomposition of hydrogen peroxide into oxygen and water was also investigated. The catalytic activity was evaluated from the consumption of hydrogen peroxide in the suspensions of the dusts in aqueous solutions of hydrogen peroxide.

Table 3 reports the percentage of H_2O_2 decomposed after 2 h of incubation. WC_{JM} appears to be a poor catalyst for this reaction, while cobalt is fairly active: the two mixtures are more active than cobalt itself, again indicating an enhancement in the activity of cobalt when in the mixture. The slight difference between WC/Co and rWC/Co may be related to a small fraction of iron present in the industrial mixture which will also contribute to the catalytic activity of the dust.[17]

Release of free radicals from suspensions in aqueous buffered solutions

The potential for free-radical release of the various samples has been determined in aqueous buffered suspension of the

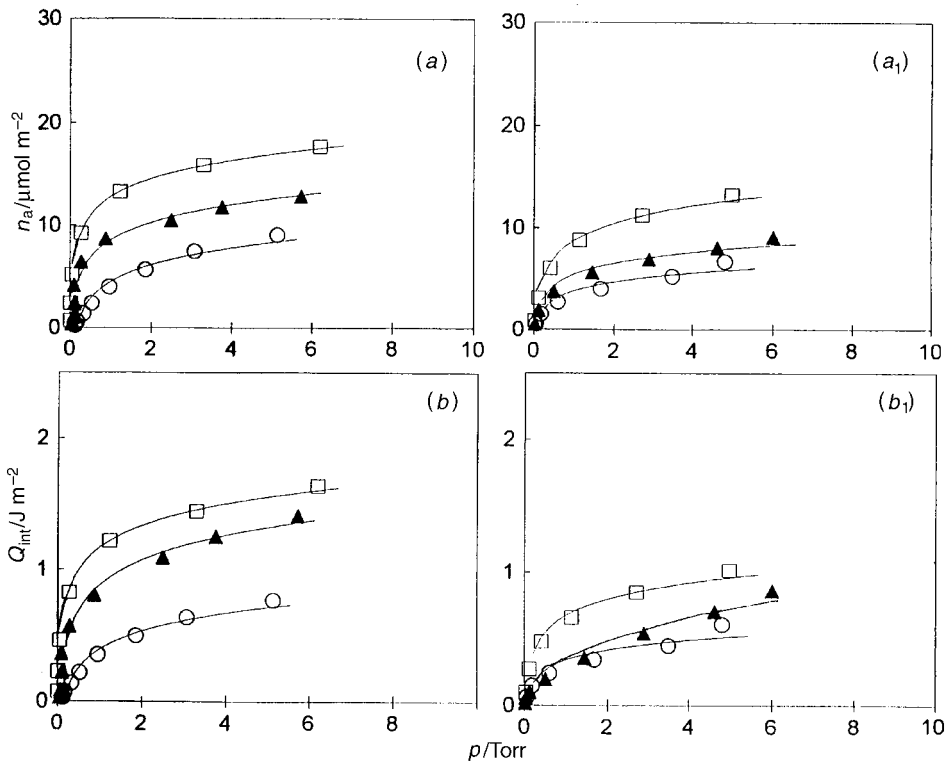

Fig. 5 Volumetric (*a*) and calorimetric (*b*) isotherms at 303 K for the total adsorption of water (ads I) on WC_{HCl} (○), WC/Co (▲), Co (□). Volumetric (a_1) and calorimetric (b_1) isotherms at 303 K for the reversible adsorption of water (ads II) on WC_{HCl} (○), WC/Co (▲), Co (□).

Table 2 Adsorption of water vapour at 303 K on WC_{HCl}, Co and WC/Co

	uptake n_a/μmol m^{-2}	integral heat Q_{int}/J m^{-2}	molar heat q/kJ mol^{-1}
WC_{HCl}	9.12	0.77	84
Co	16.91	1.60	95
WC/Co	12.35	1.37	111
WC/Co expected	9.11	0.78	86

Table 3 Catalytic decomposition of hydrogen peroxide in aqueous suspensions of the dusts; % H_2O_2 decomposed after 2 h

sample	% H_2O_2
Co	70
WC_{JM}	43
rWC/Co	91
WC/Co	98

dusts employing formate as target molecule; DMPO was used to trap the $CO_2^{\cdot -}$ radicals produced.

Fig. 6 shows the spectrum obtained for the DMPO–$CO_2^{\cdot -}$ adduct following the incubation of WC/Co in the suspension in the presence and in the absence of oxygen. The usual six-line spectrum, with intensity ratio 1 : 1 : 1 : 1 : 1 : 1, splitting constants $a_N = 15.2$G, $a_H = 18.5$ G and a g value of 2.002, is in agreement with the values reported in the literature[16] and found by some of us with asbestos.[17] Fig. 6 clearly reveals that the sample generates large amounts of DMPO–$CO_2^{\cdot -}$ adducts only in the presence of oxygen (*ca.* 13.5×10^{18} radicals l) after *ca.* 30 min.

A comparison between the activity of the industrial mixture, the reconstructed one and the two pure components is illustrated by the histograms in Fig. 7. In agreement with previously reported data[11] rWC/Co is active, while Co is virtually inactive and WC_{JM} is totally inactive. The association of carbide with Co^{II} from a $CoCl_2$ aqueous solution was also inactive.[11]

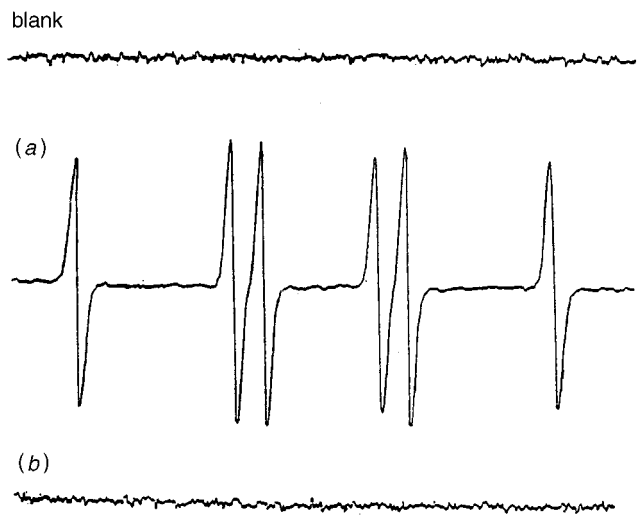

Fig. 6 EPR spectra of DMPO–$CO_2^{\cdot -}$ adducts obtained from a WC/Co suspension after 60 min in the presence (*a*) and absence (*b*) of oxygen. Blank: spectrum recorded in the absence of the solids.

The kinetics of free-radical release from a WC/Co suspension has been investigated over an extended period of time. The amount of radicals released as a function of time of incubation is shown in Fig. 8. The onset of the reaction is very slow, and only after 30 min is an appreciable amount of radicals visible. Clearly, generation of free radicals requires an induction time to take place. The reaction appears thus to be kinetically activated suggesting a mechanism involving surface reactions. An appreciable signal appears only after 30 min which increases up to a maximum after *ca.* 60 min and then decreases. From this time on a competition is established between the production and the decay of the radicals, whereby the overall intensity of the signal oscillates around the value obtained after 30 min; a signal is still present after >24 h.

In order to investigate the catalytic nature of the surface

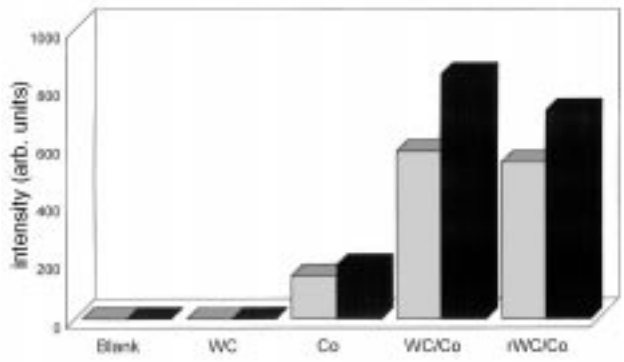

Fig. 7 Radical release from suspensions of WC, Co, WC/Co and rWC/Co, measured from the intensity of the DMPO–$CO_2^{\cdot -}$ adduct, EPR spectra recorded after 30 (light) and 60 min (dark). The values reported are averaged over several measurements.

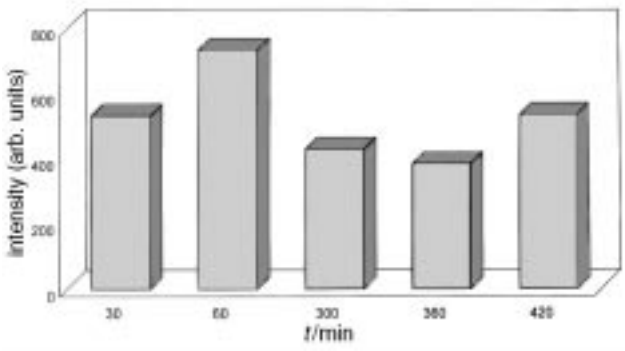

Fig. 8 Free-radical release from a WC/Co suspension as a function of time. Formate ion as target molecule, DMPO–$CO_2^{\cdot -}$ adduct. The intensity of the spectrum at subsequent time points is reported as a histogram.

active sites, spin-trapping tests were performed several times on the same sample. Results are shown in Fig. 9 where the activity of the fresh sample (I) is compared with that of a sample washed and dried after the first test (II). It is observed that, over several subsequent tests, the activity decreases but is not entirely suppressed, in contrast to asbestos, which becomes totally inactive afer the first test.[17] In the present case the signal becomes smaller after each experiment and eventually disappears. This is correlated to the progressive dissolution of cobalt, in the absence of which no free-radical release takes place (WC_{JM} is fully inactive).

The use of the formate ion does not discriminate between a mechanism whereby some radicals are generated in solution and subsequently react with the formate ion and a mechanism whereby hydrogen abstraction takes place directly at the solid/liquid interface,[12,17] since in both cases generation of the carboxylate radical takes place. The carboxylate radical $CO_2^{\cdot -}$ may thus arise from other previously formed radicals in solution (*e.g.* $^{\cdot}OH$) or *via* direct abstraction of a hydrogen atom from the formate ion at the surface of the particle.[12]

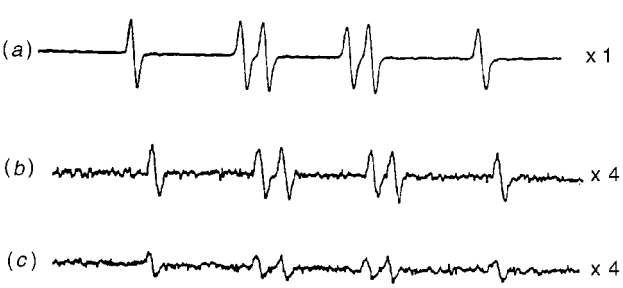

Fig. 9 Free-radical release from the same sample after washing and drying in subsequent tests. The intensities of the EPR spectra of the DMPO–$CO_2^{\cdot -}$ adduct in the first (*a*) and in the subsequent measurement (*b,c*) are compared. The spectra were recorded after 60 min.

In order to distinguish between these two possible pathways a test was performed in the absence of formate (A–OH tests). Any trace of a DMPO–$OH^{\cdot}$ adduct would indicate that the former mechanism is operating. Tests were performed using different DMPO concentrations from 50 mM up to 1 M in order to be sure that even small amounts of rapidly decaying radicals would be detectable. In all cases no DMPO adducts were formed with $^{\cdot}OH$ or $O_2^{\cdot -}$, suggesting that the radical generation takes place at the surface on some sites activated by atmospheric oxygen. To confirm this result the F–C test has also been performed in the presence of different amounts of mannitol, which is a well known scavenger of the $^{\cdot}OH$ radicals. In all cases the amount of radicals generated fell within the expected values in the absence of mannitol. Any role for the $^{\cdot}OH$ radical is thus ruled out in the proposed mechanism.

Discussion

Activation of cobalt at the carbide/cobalt interface

All the techniques employed evidence a distinct reactivity originated by the intimate contact between metallic cobalt and tungsten carbide particles. In all the experiments performed, the mixtures behave in a different way from the single components. The interface between the two in the industrial mixture is quite extensive as revealed in the high-resolution microscopy image (Fig. 1) where cobalt is spread on the carbide particle. At this interface some chemical reaction or activation occurs which may account for the specific reactivity of the mixtures. Adsorption of water vapour from the gas phase reveals that the mixture exhibits a higher adsorption capacity and a higher energy of adsorption than expected from the sum of the contributions of the two components. This can be only explained by the creation, upon contact of the particles, of strong hydrophilic sites, probably cobalt ions partially bound to the carbide surface, with residual capability either of strong coordination to water molecules or ability to dissociate water into surface hydroxyl groups. The distinct behaviour of the mixture leads to irreversible adsorption sites (compare ads I and ads II in Fig. 5). This type of adsorption on oxides is characteristic of strong coordination of water on exposed metal ions (strong Lewis acids), or of the dissociation of water which yields surface hydroxyl groups.[21]

Weakly coordinated cobalt ions may also be responsible for the higher catalytic activity of the mixture than of pure cobalt in the hydrogen peroxide disproportionation (Table 3).

We may therefore hypothesize that the thin layer of oxide, which originates from cobalt particles exposed to air, when in contact with the carbide surface, might create a dispersion of cobalt ions at the interface which, because of weak coordination, are more reactive in several surface reactions than ions in the thin oxide layer over metallic cobalt.

Reactivity of the solids in phosphate-buffered aqueous suspension

Incubation of the mixed dusts in a phosphate-buffered aqueous solution brings about dramatic changes involving both the solid and the solution. Cobalt is progressively oxidixed to cobalt(II) ions to a much larger extent than for pure cobalt. Correspondingly, free radicals are released into the solution, and the micromorphology changes from dispersed particles of *ca.* 50 μm diameter to larger (300–400 μm) smooth aggregates. As free-radical generation does not take place under non-aerobic conditions (Fig. 6) and much less cobalt is oxidized and brought into solution, the most likely mechanism is that shown in Fig. 10. The electrons originating from the oxidation of cobalt migrate to the carbide surface where they reduce

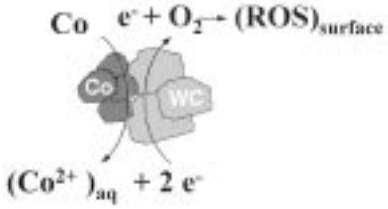

Fig. 10 Proposed mechanism for oxygen reduction by a mixture of cobalt (Co) and tungsten carbide (WC) particles. When both particles are in close contact, electrons (e^-) provided by cobalt are transferred to the surface of tungsten carbide where atmospheric oxygen is activated into a surface-reactive oxygen species (ROS), which in turn generates free radicals *via* abstraction of a hydrogen atom. Cobalt is progressively oxidized and passes into solution as Co^{2+}.

atmospheric oxygen to some surface-reactive oxygen form, as may be evidenced by its reaction with the formate ion, yielding carboxylate radicals. As long as some metallic cobalt is present the reaction proceeds until all the metal has been brought into solution. The presence of phosphate ion, which has a high affinity for cobalt on the one hand facilitates the oxidation of the metal, and on the other, because of the low solubility of the phosphate, may be implied in the aggregation into large smooth particles seen in the SEM micrographs.

Although in some cases free-radical generation from aqueous solutions of Co^{II} has been reported,[22–25] there is sufficient evidence in our present and previous data[11] that Co^{II} is not implied in the formation of the carboxylate radical.

All the experiments performed indicate that free-radical generation takes place at the solid/liquid interface *via* direct abstraction of a hydrogen atom from the formate ion, without any $^{\cdot}OH$ intermediate. Atmospheric oxygen is required to lead to oxidation of the active site at the carbide surface.

Implication of surface reactivity in the health effects of the inhaled dusts

The toxicity of inhaled hard metal particles may be explained by the surface reactivity which originates upon contact between the two components. *In vivo* the respirable fraction of the particles will be inhaled and will undergo in body fluids (cellular and extracellular) similar reactions to those described, although at a lower rate.

The mineralogical analysis of biopsy materials has revealed tungsten accumulation but insignificant cobalt except for grinders exposed for long periods of time.[6] No comments are reported on the size of the particles found.

Collaborative research is in due course to investigate whether morphologicals transformations *in vivo* parallel what was seen in our experiments with buffered solutions. Enlargement of deposited particles *in vivo* would involve a lower clearance rate and hence a higher pathogenicity.

A continuous release of free radicals at the site of deposition of the particle will then take place which may overwhelm the body defences and cause persistent inflammation. This could also offer a reasonable explanation for the fact that only a small proportion of workers exposed to hard metal powders develop the disease. It may be speculated that individuals with a lower antioxidant defence are more susceptible to the toxic effects of the inhaled hard metal particles.[26]

Conclusions

The different techniques employed indicate that multicomponent dusts may react in a different way than the single components. This effect appears related to mere contact between microsized metallic particles and a carbide with semiconductor properties. A mutual activation may take place, which, as in the present case, may originate an enhanced reactivity and a health hazard higher than that due to the single components alone. This is very relevant to any study concerning the environmental hazard of solid particulates, as, obviously, most urban particulates consist of complex mixtures of various polluting compounds.

The work was supported by the Commission of the European Communities (Directorate General XII-Research and Technological Department-Environment) project no. PL931359. The authors are indebted to Dr. D. Lison for encouragement and fruitful discussions and are grateful to Dr. Gianmario Martra for helping in the TEM investigations and interpretation.

References

1 A. O. Bech, M. D. Kipling and J. C. Heather, *Br. J. Ind. Med*., 1962, **19**, 239.
2 D. W. Cugell, *Clin. Chest Med*., 1992, **13**, 269.
3 D. Lison and R. Lauwerys, *Toxicol. Lett*., 1992, **60**, 203.
4 G. Lasfargues, P. Wild, J. J. Moulin, B. Hammon, B. Rosmorduc, B. Rondeau du Noyer, M. Lavandier and J. Moline, *Am. J. Ind. Med*., 1994, **26**, 585.
5 B. Nemery, *Eur. Respir. J*, 1990, **3**, 202.
6 D. Lison, *Crit. Rev. Toxicol*., 1996, **26**, 585.
7 D. Lison and R. Lauwerys, *Environ. Res*., 1990, **52**, 187.
8 G. Lasfargues, D. Lison, P. Maldague and R. Lauwerys, *Toxicol. Appl. Pharmacol*., 1992, **112**, 41.
9 D. Lison and R. Lauwerys, *Arch. Toxicol*., 1994, **68**, 528.
10 G. Lasfargues, C. Lardot, M. Delos, R. Lauwerys and D. Lison, *Environ. Res*., 1996, **69**, 108.
11 D. Lison, P. Carbonelle, L. Mollo, R. Lauwerys and B. Fubini, *Chem. Res. Toxicol*., 1995, **8**, 600.
12 B. Fubini, in *Mechanisms of Fibre Carcinogenesis*, ed. A. B. Kane, P. Boffetta, R. Saracci and J. D. Wilbourn, Lyon, 1996, p.35.
13 H. A. Mottola, B. E. Simpson and G. Gorin, *Anal. Chem*., 1970, **42**, 410.
14 E. G. Janzen and B. J. Blackburn, *J. Am. Chem. Soc*., 1968, **90**, 5909.
15 C. Mottley and R. P. Mason, *Biol. Magn. Reson*., 1989, **8**, 489.
16 R. Zalma, L. Bonneau, M. C. Jaurand, J. Guignard and H. Pezerat, *Can. J. Chem*., 1987, **65**, 2338.
17 B. Fubini, L. Mollo and E. Giamello, *Free Radical Res*., 1995, **23**, 593.
18 B. Fubini, *Thermochim. Acta*, 1988, **135**, 19.
19 B. Fubini, V. Bolis, A. Cavenago, E. Garrone and P. Ugliengo, *Langmuir*, 1993, **9**, 2712.
20 V. Bolis, B. Fubini, L. Marchese, G. Martra and D. Costa, *J. Chem. Soc., Faraday Trans.,* 1991, **87**, 497.
21 B. Fubini, V. Bolis, M. Bailes and F. S. Stone, *Solid State Ionics*, 1989, **32**/**33**, 258.
22 C. P. Moorhouse, B. Halliwell, M. Grootveld and J. M. C. Gutteridge, *Biochem. Biophys. Acta*, 1985, **843**, 261.
23 M. B. Kadiiska, K. R. Maples and R. P. Mason, *Arch. Biochem. Biophys*, 1989, **275**, 98.
24 P. M. Hanna, M. B. Kadiiska and R. P. Mason, *Chem. Res. Toxicol*., 1992, **5**, 109.
25 Y. Mao, K. J. Liu, J. J. Jiang and X. Shi, *J. Toxicol. Environ. Health*, 1996, **47**, 61.
26 D. Lison, R. Lauwerys, M. Demedts and B. Nemery, *Eur. Respir. J*., 1996, **9**, 1024.

Paper 7/00846E; *Received 5th February*, 1997